# Stretching and compressing of short laser pulses by chirped volume Bragg gratings: analytic and numerical modeling

Sergiy Kaim
Sergiy Mokhov
Boris Y. Zeldovich
Leonid B. Glebov

# Stretching and compressing of short laser pulses by chirped volume Bragg gratings: analytic and numerical modeling

Sergiy Kaim, Sergiy Mokhov, Boris Y. Zeldovich, and Leonid B. Glebov*
University of Central Florida, CREOL–The College of Optics & Photonics, 4000 Central Florida Boulevard, Orlando, Florida 32816

**Abstract.** The theory of stretching and compression of short light pulses by chirped volume Bragg gratings (CBGs) is reviewed based on spectral decomposition of short pulses and on wavelength-dependent coupled wave equations. Analytic theory of diffraction efficiency of CBG with constant chirp and approximate theory time-delay dispersion is presented. Comparison of approximate analytic results with exact numeric coupled-wave modeling shows excellent agreement for smooth heterogeneities of CBGs. © *The Authors. Published by SPIE under a Creative Commons Attribution 3.0 Unported License. Distribution or reproduction of this work in whole or in part requires full attribution of the original publication, including its DOI.* [DOI: 10.1117/1.OE.53.5.051509]

## 1 Introduction

Chirped pulse amplification[1] is the main approach for high-power/high-energy ultrashort laser pulse' generation. It is achieved by stretching ultrashort laser pulses. Those stretched pulses have a much lower value of instantaneous power and, therefore may be amplified by broadband laser amplifiers without damaging the medium. Amplified chirped pulses may then be directed to the compressing element, which allows collection of all spectral components back into ultra-short pulse, but with higher energy. The conventional way for doing this is the use of a pair of diffracting gratings for both stretching and compression (Treacy stretchers and compressors[1]). An especially elegant idea was suggested and implemented by Galvanauskas et al.[2,3] with the use of chirped fiber Bragg gratings, which are gratings with a gradually varied period along the fiber. It is possible to use the same grating for compression, and stretching stage, but to illuminate it from the opposite end. In this case, the influence of smooth heterogeneities of time-delay dispersion (TDD) at the stretching stage, $T_{str}(\lambda)$, is compensated for by those of the compression stage, so that $T_{str}(\lambda) + T_{compr}(\lambda) \approx$ const. A similar performance was demonstrated with the use of chirped volume Bragg gratings (chirped VBGs or CBGs), which are produced by holographic recording in the bulk of photo-thermo-refractive (PTR) glass and have dramatically higher apertures when compared with those of fiber gratings.[4] Recent development of VBGs based on PTR glass[5] allowed for operation of stretching-compression schemes at much higher values of power, see for example, Ref. 6.

The present paper is devoted to the development of numerical and analytic tools for the study of stretching and compression by volume CBGs. While this analysis is applicable for any volume CBG, the examples shown in this paper are based on CBGs recorded in PTR glass.

## 2 Basic Scheme and System of Equations, Definition of Chirp, and Time-Delay Dispersion

The basic scheme of stretching, amplification of stretched pulse, and subsequent recompression back into short pulse by means of a volume CBG is presented in Fig. 1. Due to gradual variation of CBG period in the $z$ direction, different spectral components of an incident pulse are reflected from different parts of the CBG and, therefore, have different delays. After amplification, the stretched pulse is launched to the same CBG from the opposite side and compressed back to its original width. In this work, we consider the amplifier as a linear device that does not affect any parameters of a laser pulse but power. Therefore, we assume that a CBG-reflected stretched pulse is transmitted from the cross-section at the front surface of the CBG ($z = 0$) to the opposite end of the same CBG ($z = L$), without any additional distortions.

We assume that the dielectric permittivity and magnetic permeability of CBG depend on coordinate $z$ as

$$\varepsilon(z) = (n_0^2 + 2n_0\delta n(z) + O(\delta n)^2) \cdot \varepsilon_{vac}, \qquad \mu \equiv \mu_{vac},$$

(1)

where $\delta n(z)$ is the variation of refractive index. Then the equation for the complex amplitudes $A(z)$ and $B(z)$ of monochromatic component of electric field

$$E_{real}(z, t) = \frac{1}{2}\{\exp(-i\omega t)[A(t)\exp(ikz) + B(t) \\ \times \exp(-ikz)] + compl.conj.\}$$

(2)

with $k = \omega n/c$, $n_0 \equiv n(\omega)$ is

$$\frac{d^2}{dz^2}[A(z)e^{ikz} + B(z)e^{-ikz}] + \left(\frac{\omega}{c}\right)^2[n_0^2 + 2n_0\delta n(z)] \\ \cdot [A(z)e^{ikz} + B(z)e^{-ikz}] = 0,$$

(3)

*Address all correspondence to: Leonid B. Glebov, E-mail: lbglebov@mail.ucf.edu
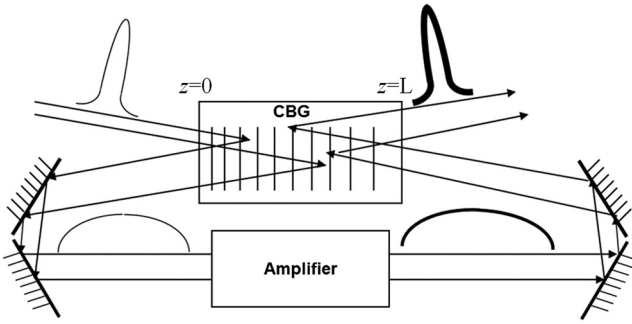
**Fig. 1** Basic scheme of stretching–amplification–compression via Chirped Bragg grating (CBG).

where the terms of the order of $O(\delta n)^2$ were ignored. We also assume that the spatial variation of the refractive index $\delta n(z)$ has the form

$$\delta n(z) = n_2(z) + n_1(z) \cos[Qz + \psi(z)]. \qquad (4)$$

Here, smooth heterogeneity $n_2(z)$ and spatial modulation $n_1(z)$ are small in comparison with $n_0$ and are relatively slow varying functions of $z$; $\psi(z)$ is a differentiable function, and $Q$ (rad/m) has the value close to $2k$, see Eq. (13). (It should be emphasized that our notation $n_2(z)$ for the smooth correction to the background refractive index has nothing to do with the nonlinearity of refractive index.) In the standard approach of slow varying envelope approximation (SVEA), one should ignore second derivatives of slowly varying amplitudes $A(z)$ and $B(z)$, keep the resonant terms $\propto \exp(ikz)$ and $\propto \exp(-ikz)$ only, and equalize each of them to zero. As a result, one gets the following system of coupled equations:

$$\frac{dA}{dz} = i(\omega/c)n_2(z) \cdot A(z) + i(\omega/2c)n_1(z)$$
$$\times \exp[iQz - 2ikz + i\psi(z)] \cdot B(z),$$
$$\frac{dB}{dz} = -i(\omega/2c)n_1(z) \exp[-iQz + 2ikz - i\psi(z)]$$
$$\cdot A(z) - i(\omega/c)n_2(z) \cdot B(z). \qquad (5)$$

It is convenient now to introduce new amplitudes $a(z)$ and $b(z)$, defined by

$$a(z) = A(z) \exp\left\{\frac{i}{2}[(2k - Q)z - \psi(z)]\right\},$$
$$b(z) = B(z) \exp\left\{\frac{-i}{2}[(2k - Q)z - \psi(z)]\right\}. \qquad (6)$$

Then for these small amplitudes $a(z)$ and $b(z)$, one gets our system in the form

$$\frac{d}{dz}\begin{bmatrix} a(z) \\ b(z) \end{bmatrix} = \hat{V}(z)\begin{bmatrix} a(z) \\ b(z) \end{bmatrix},$$
$$\hat{V}(z) = \begin{bmatrix} i\nu(z) & i\kappa(z) \\ -i\kappa(z) & -i\nu(z) \end{bmatrix}, \qquad (7)$$

Here $\nu(z)$ is the local value of detuning, measured in (rad/m), and $\kappa(z)$ is the local strength of coupling, of dimensions $(1/m)$

$$\nu(z) = \left(\frac{\omega}{c}\right)n_2(z) + \frac{2k - Q - d\psi(z)/dz}{2},$$
$$\kappa(z) = \left(\frac{\omega}{c}\right)\frac{n_1(z)}{2}. \qquad (8)$$

Possible background absorption in the medium with coefficient $\alpha(1/m)$, for intensity $I(z) \sim \exp(-\alpha z)$, may be described by purely imaginary $n_2(z)$, namely $n_2(z) = i\lambda\alpha/4\pi$.

Solution of the linear system of ordinary differential equations [Eq. (7)] may be represented as the solution of the Cauchy problem, where both boundary values are known at the same point, e.g., at $z = 0$. Linearity of the system allows writing.

$$\begin{bmatrix} a(z) \\ b(z) \end{bmatrix} = \begin{bmatrix} M_{aa}(z) & M_{ab}(z) \\ M_{ba}(z) & M_{bb}(z) \end{bmatrix} \cdot \begin{bmatrix} a(0) \\ b(0) \end{bmatrix},$$
$$\frac{d\hat{M}(z)}{dz} = \hat{V}(z)\hat{M}(z),$$
$$\hat{M}(0) = \begin{bmatrix} 1 & 0 \\ 0 & 1 \end{bmatrix}. \qquad (9)$$

Actual boundary conditions for the reflection problem are usually prescribed at the opposite ends of CBG; for example

$$a(z = 0) = 1, \qquad b(z = L) = 0, \qquad (10)$$

where we assumed unit amplitude of incident wave $a$ at the beginning $z = 0$ of CBG and no incident wave $b$ at the end $z = L$ of CBG. Then the reflection and transmission amplitudes are found by imposing the conditions in Eq. (10).

$$r(b \leftarrow a) \equiv \frac{b(0)}{a(0)} = -\frac{M_{ba}(L)}{M_{bb}(L)},$$
$$t(a \rightarrow a) \equiv \frac{a(L)}{a(0)} = \frac{M_{bb}(L)M_{aa}(L) - M_{ba}(L)M_{ab}(L)}{M_{bb}(L)}. \qquad (11)$$

The determinant of the matrix $\hat{M}(z)$ from Eq. (9), which is present in the numerator of Eq. (11), is unity as the consequence of Eq. (7), even in the presence of absorption. This allows additional checking of the accuracy of numeric integration of those equations.

The amplitude of reflection and transmission for the opposite boundary conditions may be expressed through the elements of the same matrix $\tilde{M}(L)$.

$$r(b \rightarrow a) \equiv \frac{a(L)}{b(L)} = \frac{M_{ab}(L)}{M_{bb}(L)},$$
$$t(b \leftarrow b) \equiv \frac{b(0)}{b(L)} = \frac{1}{M_{bb}(L)}, \qquad (12)$$

which is especially convenient for the case when one uses the same CBG both for stretching and for recompression.

Subsequently, we neglect the $n_2(z)$ term. Then, equating the local value of detuning $\nu(z)$ to zero, one can find the position $z_B(\lambda)$ of the point of exact Bragg resonance for the given vacuum wavelength $\lambda$.

$$\nu(z_B) = 0 \Rightarrow \frac{2\pi n(\lambda)}{\lambda} = \frac{2\pi n(\lambda_0)}{\lambda_0} + \frac{1}{2}\frac{d\psi}{dz}. \qquad (13)$$

Here $\lambda_0$ is the central wavelength defined by basic parameter of CBG: $Q = 4\pi n(\lambda_0)/\lambda_0$, with $Q$ defined by Eq. (4). This condition allows connecting spectral chirp parameter $d\lambda/dz_B$ of CBG with the second derivative of the phase correction $\psi(z)$. Indeed, one has to assume $\lambda = \lambda(z)$ in Eq. (13) and take $z$-derivative of the left- and right-hand sides of that equation. As a result, one gets

$$\frac{d\lambda}{dz_B} = -\frac{\lambda^2}{4\pi n_{gr}(\lambda)}\frac{d^2\psi}{dz^2}, \qquad n_{gr}(\lambda) = n(\lambda) - \lambda\frac{dn}{d\lambda}. \qquad (14)$$

Here the expression for $n_{gr}$ is an alternative form of denoting group velocity, $v_{gr} = d\omega/dk = c/n_{gr}$ and $n_{gr} = n(\omega) + \omega(dn/d\omega) \equiv n(\lambda) - \lambda(dn/d\lambda)$. Constant chirp ($d\lambda/dz_B = $ const) corresponds to $\psi(z) = \beta \cdot (z - 0.5L)^2$, where the mid-point $z = 0.5L$ of CBG with length $L$ has resonant wavelength $\lambda_0$. Indeed,

$$\psi(z) = \beta \cdot (z - 0.5L)^2 \Rightarrow \frac{d\lambda}{dz_B} = -\frac{\lambda^2}{2\pi n_{gr}}\beta. \qquad (15)$$

In the approximation of unchanged group velocity $v_0 = c/n_{gr}$, the value of time-delay in the stretching process as a function of wavelength $\lambda$ is

$$T_1(\lambda) \equiv \text{TDD}(\lambda) \approx 2[z_B(\lambda) - z_1]n_{gr}/c. \qquad (16)$$

We will see below (Fig. 7 in Sec. 5.3) that this formula yields a reasonable result for CBG with low efficiency only.

## 3 Analytic Expression of Diffraction Efficiency of CBG

Consider first a weak CBG for which the first order of perturbation theory is valid. In the zeroth approximation and at $n_2 \equiv 0$, one can take $A(z) \approx 1$ for all $z$. Then for the reflection amplitude coefficient, one gets from Eq. (5)

$$r(A \to B) = B(-\infty) = i\kappa \int_{-\infty}^{\infty} \exp[-i\psi(z)]dz, \qquad (17)$$

which, for $\psi(z) = \beta \cdot (z - 0.5L)^2$, yields explicit value of

$$|r|^2 \approx \pi|\kappa|^2/|\beta|. \qquad (18)$$

An analytic expression has been derived in Ref. 8, which is valid for any strenth of coupling. It may be simplified for constant chirp profile of the grating, with the use of Eq. (15) to:

$$|r|^2 = 1 - \exp(-\pi|\kappa|^2/|\beta|), \qquad |t|^2 = 1 - |r|^2. \qquad (19)$$

Derivation of this expression, see Refs. 7 and 8, is similar to the calculation of quantum-mechanical transmissivity of parabolic potential barrier, see Ref. 9, and will not be discussed here. To go over the rather heavy derivation of Eq. (19) from Refs. 8 and 7, we suggest using the known structure of Eq. (19) and checking all the coefficients in it via the first-order perturbation result [Eq. (18)]. Actual

numerical modeling (see below) confirmed the validity of Eq. (19) with great accuracy, especially for apodized CBG, where spatial refractive index modulation comes smoothly to zero at the ends of CBG in this particular modeling, see Eq. (40).

## 4 Approximate Expression for Time-Delay Dispersion

Approximate evaluation of TDD may be done on the basis of assumption of slowly varying behavior of the coefficients $\kappa = k(z)$ and $\nu = \nu(z)$ in Eq. (7). We take the SVEA equations in the symmetric form.

$$\frac{d}{dz}\begin{pmatrix} a \\ b \end{pmatrix} = \hat{V}\begin{pmatrix} a \\ b \end{pmatrix}, \quad \hat{V} = \begin{pmatrix} i\nu & i\kappa^* \\ -i\kappa & -i\nu \end{pmatrix}. \qquad (20)$$

In the assumption of $\nu = $ const, $\kappa = $ const, the solution of the form $(a, b) = \exp(pz)(a_0, b_0)$ exists. From that we get the result for two eigenvalues of matrix $\hat{V}$.

$$p_{1,2} = \pm i\mu, \quad \mu = +\sqrt{\nu^2 - |\kappa|^2}. \qquad (21)$$

We define the positive root as the one for which, in the region $|\kappa| < |\nu|$, the real square root $\mu = +\sqrt{\nu^2 - |\kappa|^2}$ satisfies the condition $\mu/|\mu| = \nu/|\nu|$; in other words, the sign of $\mu$ is the same as the sign of $\nu$ in that region where propagation is not forbidden. Eigenvectors for $p_1 = +i\mu$ and for $p_2 = -i\mu$ are, respectively,

$$\begin{pmatrix} a_1 \\ b_1 \end{pmatrix} = \text{const}_1\begin{pmatrix} 1 \\ -\kappa/(\mu + \nu) \end{pmatrix},$$
$$\begin{pmatrix} a_2 \\ b_2 \end{pmatrix} = \text{const}_2\begin{pmatrix} -\kappa^*/(\mu + \nu) \\ 1 \end{pmatrix}. \qquad (22)$$

Group velocity of the wave $a$ in the absence of coupling, $|\kappa| = 0$, is taken as $v_a = v_0$, while group velocity of the wave $b$ is taken as $v_b = -v_0$. The general expression for the group velocity in the presence of both constant values $\nu$ and $\kappa$ for a given mode may be intuitively written as

$$v_{gr} = P[\text{Watt/m}^2]/U[\text{Joule/m}^3], \qquad (23)$$

where $P$ is the Poynting vector and $U$ is the energy density. Assuming $P = |a|^2 - |b|^2$, $U = \text{const} \cdot (|a|^2 + |b|^2)$ and checking the case of $|\kappa| = 0$, we get $\text{const} = 1/v_0$. Thus, in general case, group velocity in the presence of grating becomes

$$v_{\text{group}} = v_0\frac{|a|^2 - |b|^2}{|a|^2 + |b|^2}. \qquad (24)$$

In the approximation of constant (or reasonably slow varying) $\nu$ and $\kappa$, one gets for mode #1 (a predominantly $a$-wave) and for mode #2 (a predominantly $b$-wave)

$$v_1 = (v_a) = v_0\left|\frac{\mu}{\nu}\right|, \quad v_2 = (v_b) = -v_0\left|\frac{\mu}{\nu}\right|. \qquad (25)$$

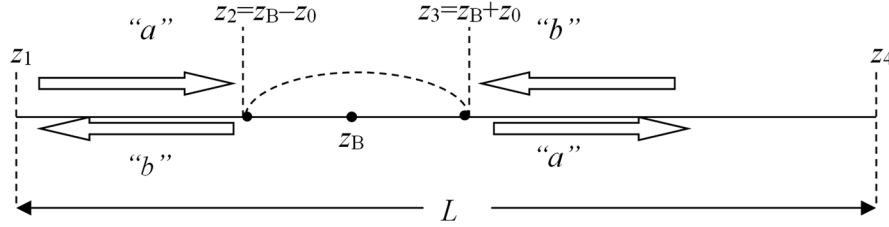We take those expressions as approximations for group velocities of incident and reflected waves in the use of

**Fig. 2** Transmitting and reflecting wave propagation in CBG. Here $L$ is the total thickness of CBG; $z = z_2$ is the point where the input wave $a$ of the given frequency $\omega = 2\pi c/\lambda$ hits the region forbidden for propagation (marked by curved dashed line).

CBG for the stretcher-compressor scheme and verify the degree of their validity by comparison with results of direct wave modeling of CBG, Sec. 5.

In this approximate approach (Fig. 2), the incident wave $a$ (the one to be stretched by CBG) propagates from the point $z = z_1$ of the left boundary of CBG to the left point $z = z_2$ inside CBG, where decisive reflective transformation of $a$ into $b$ takes place. The points $z = z_2$ and $z = z_3$ are defined by the condition $\nu(z_{2,3}, \lambda) = \pm|\kappa|$. In CBG approximated by constant chirp, $\nu(z, \lambda) = \beta \cdot [z - z_B(\lambda)]$, those points are symmetrically positioned around $z_B(\lambda)$, i.e., around perfect Bragg-resonant point.

$$z_2 = z_B(\lambda) - z_0, \quad z_3 = z_B(\lambda) + z_0, \quad z_0 = |\kappa|/|\beta|. \quad (26)$$

After the decisive reflection from the point $z = z_2$, incident wave of type $a$ gets transformed into reflected wave of type $b$. Total time-delay due to propagation from the entrance $z = z_1$ to reflection point $z = z_2$ and back is

$$T_1(\lambda) \equiv T(z_1 \to z_2 \to z_1)[\text{second}] = 2\int_{z_1}^{z_2} [\mathrm{v}(z)]^{-1}dz, \quad (27)$$

where $\mathrm{v}(z) = \mathrm{v}_0 \cdot |\mu(z)/\nu(z)|$ as a consequence of Eqs. (22) and (24). At the compression stage, the wave enters CBG through the cross-section $z = z_4$ and propagates in the $b$-form down to $z = z_3$, and after the reflection, it propagates back to $z = z_4$. The corresponding round-trip delay time of this stage is given by

$$T_2(\lambda) \equiv T(z_4 \to z_3 \to z_4)[\text{second}] = 2\int_{z_3}^{z_4} [\mathrm{v}(z)]^{-1}dz, \quad (28)$$

where again $\mathrm{v}(z) = v_0 \cdot |\mu(z)/\nu(z)|$. For a general $z$-dependence of $\nu(z)$ and $\kappa(z)$, one should numerically find $z_B(\lambda), z_2(\lambda), z_3(\lambda)$ and numerically calculate the corresponding integrals. Calculation can be done analytically for constant chirp and constant $\kappa$.

$$\nu(z) = \beta \cdot [z - z_B(\lambda)], \quad z_1 = 0, \quad z_4 = L,$$
$$z_B(\lambda) = \frac{L}{2} + \left(\frac{d\lambda}{dz}\right)^{-1} \cdot (\lambda - \lambda_0). \quad (29)$$

Equation (15) yields the expression for $d\lambda/dz$. Here $\lambda_0$ is the central wavelength of CBG. In that case, $z_2 = z_B(\lambda) - z_0$, $z_3 = z_B(\lambda) + z_0, z_0 = |\kappa|/\beta$, and integrals may be found analytically.

$$T(z_1 \to z_2 \to z_1) = \frac{2}{\mathrm{v}_0}\sqrt{[z_B(\lambda)]^2 - z_0^2},$$
$$T(z_4 \to z_3 \to z_4) = \frac{2}{\mathrm{v}_0}\sqrt{[L - z_B(\lambda)]^2 - z_0^2}, \quad (30)$$

$$T_{\text{cycle}} \equiv T(z_1 \to z_2 \to z_1) + T(z_4 \to z_3 \to z_4)$$
$$= \frac{2}{\mathrm{v}_0}\left\{\sqrt{[z_B(\lambda)]^2 - z_0^2} + \sqrt{[L - z_B(\lambda)]^2 - z_0^2}\right\}. \quad (31)$$

In the case when both $z_0 \ll z_B(\lambda)$ and $z_0 \ll L - z_B(\lambda)$, one can expand $T_{\text{cycle}}(\lambda)$ in terms of small ratio $z_0/L$.

$$T_{\text{cycle}}(\lambda) \approx \frac{1}{\mathrm{v}_0}\left\{2L - \frac{4z_0^2}{L}\frac{L^2}{L^2 - 4[z_B(\lambda) - L/2]^2}\right\}. \quad (32)$$

One should take the value of $T_{\text{cycle}}$ from Eqs. (31) or (32) above and then average the expression over the spectral content of the pulse in question. As an even more crude estimate, one may try to take the value of $T_{\text{cycle}}$ at $|z_B - L/2| \ll z$, and then the formula for time-delay of the peak of recompressed pulse becomes

$$T_{\text{cycle}} \approx \frac{1}{\mathrm{v}_0}\left(2L - \frac{4z_0^2}{L}\right). \quad (33)$$

It is worth discussing separately two effects that influence the delay time of the cycle stretching–recompression.

The first one is that the round-trip length of the stretching process is shorter than $2[z_B(\lambda) - z_1]$ by the thickness of forbidden zone: $2z_0 = 2|\kappa/\beta|$, see Fig. 2. This leads to a shorter delay time of the stretching–recompression cycle: shorter by approximately $(4z_0/\mathrm{v}_0)$, i.e., of the first order in $z_0$.

The second effect is due to considerable ($\sim$50% and more) decrease of group velocities in the vicinity of reflection points $z = z_2$ and $z = z_3$. The thickness of this vicinity is of the order of $z_0$. Thus, this second effect results in a longer delay time, also of the first order in $z_0$.

What is truly remarkable is that these two effects compensate each other in the first order in $z_0$. The resulting delay time does decrease (in comparison with $2L/\mathrm{v}_0$), but in the second order in the coupling constant, i.e., proportionally to $z_0^2$.

A monochromatic wave stretches in time from $t = -\infty$ to $t = +\infty$. One can define time delay dispersion TDD($\lambda$) for the quasi-monochromatic packet with the wavelength $\lambda$. Many sources advise to one calculate the phase of reflection coefficient $\varphi(\lambda) = \arg(r(\lambda))$ and postulate that

$$\frac{d\omega}{d\lambda} = -\frac{2\pi c}{\lambda^2}, \quad \text{TDD}(\lambda) = \frac{d\varphi}{d\omega} \equiv \frac{d\varphi}{d\lambda}\frac{d\lambda}{d\omega} \equiv -\frac{\lambda^2}{2\pi c}\frac{d\varphi(\lambda)}{d\lambda}.$$
(34)

Our numeric modeling shows that this is valid for large modulation of $\varphi(\lambda)$ only, $|\varphi| \gg 1$.

## 5 Numerical Modeling

### 5.1 *Parameters of Numerical Modeling*

We have developed the program for numerical modeling of the scheme presented in Fig. 1 with the use of Mathematica software package. In our approach, the fields of all pulses were decomposed into time Fourier series via discrete Fourier transform (DFT) subroutine. The discrete index $j$ in DFT programs takes only non-negative values in the range $0 < j < N - 1$, where $N$ is the total number of points (either in time domain or in frequency domain). For that reason the frequency of an individual component was related to that index $j$ by

$$\omega_j = \omega_{\text{central}} + (2\pi/T_{\text{total}}) \times \text{phys}(j),$$

$$\text{phys}(j) = \begin{cases} j, & \text{if } 0 < j < N/2; \\ j - N, & \text{otherwise} \end{cases}.$$
(35)

In that manner, we account for both positive and negative values of frequency detuning. Meanwhile discrete time points were numbered just as

$$t_j = t_{\text{initial}} + j \cdot \Delta, \quad \Delta = T_{\text{total}}/N.$$
(36)

Here $T_{\text{total}}$ is the total time interval under consideration. Average refractive index of PTR glass was taken for each wavelength $\lambda_j = 2\pi c/\omega_j$ as either constant value $n = 1.4891$ (for central wavelength $\lambda_{\text{central}} = 1.06$ μm) or from Sellmeier formula for that glass.[10] The system of ordinary differential equations was integrated numerically for each frequency $\omega_j$. Sometimes it was advantageous to divide all the integration length $L$ (thickness of CBG) into four separate regions, with accuracy goal achieved for each region independently. Examples below are demonstrated mostly for $L = 0.1$ m ($\equiv 10$ cm) and constant chirp parameter $\beta = 8.10^4$ rad/m$^2$ from Eq. (15). Value of coupling constant $|\kappa|$ was chosen via dimensionless parameter $S = |\kappa|L$, with $S$ varying from 15 to 150.

### 5.2 *Modeling of Stretching–Compressing by CBG with Imperfections*

It should be noted that CBGs with large apertures and long stretching times[4,6,11] show some spatial variations of phase resulting from optical aberrations in a holographic recording system and optical homogeneity of a recording material (PTR glass). This is why, among other results of our numerical modeling of stretching–compression process, we would like to discuss here the influence of small and very inhomogeneous variations of phase of the grating. Equation (13) allows finding the position $z_B(\lambda)$, where formal Bragg condition is satisfied for a given wavelength $\lambda$. We took a small oscillatory addition to the phase, $\delta\psi = a \cos \gamma z$, where $\gamma[1/\text{meter}] = 2\pi/\Lambda_1$ and $\Lambda_1$ is the period of perturbations. Since the term $d\psi/dz$ is present in the right-hand side of

Eq. (13), the equation for detuning $z_B(\lambda)$ becomes

$$\frac{2\pi n(\lambda)}{\lambda} = \frac{2\pi n(\lambda_0)}{\lambda_0} - \beta(z_B - b) + a\gamma \sin \gamma z_B.$$
(37)

If $a\gamma^2$ is larger than $2|\beta|$, then there is a possibility that Eq. (37) has several solutions $(z_B)_1, (z_B)_2, \ldots$ for the given wavelength $\lambda$. Then application of the simplest formula

$$\text{TDD}(\lambda) \approx 2(z_B(\lambda) - z_1)/\text{v}_0,$$
(38)

yields multivalued $\text{TDD}(\lambda)$ and gives a suspicion of low-quality recompression, to say nothing about peculiar oscillations, which are even more severe in the stretched pulse. However, the results of our numerical modeling show for phase modulation

$$\delta\psi = a \cos(\gamma z) \cdot \exp(-(z - 0.5\,L)^2/d^2), \quad d = L/4$$
(39)

that if the amplitude $2a$ (top to bottom) is moderately small, e.g., $2a \leq 0.4$ rad, the influence of formally multivalued feature of $\text{TDD}(\lambda)$ from Eq. (38) is not important. In particular, Fig. 3 shows z-dependence of Bragg resonant wavelength detuning (in nanometers) for particular perturbation of the phase given by Eq. (39). Actual wave modeling of stretching by perturbed CBG was done for $L = 0.1$ m and $\beta = 8 \cdot 10^4$ rad/m$^2$, coupling coefficient $|\kappa| = S/L$, and $S = 30$. Additional modulation $\delta\psi$ from Eq. (39) was taken with the parameters $2a = 0.4$ rad, $\gamma = 1405$ rad/m. so that $a\gamma^2/2\beta = 2.47$, and the condition of multivalued function $\text{TDD}(\lambda)$ from Eq. (38) was satisfied. Stretching and compression of incident Gaussian pulse with $\tau_0(\text{HW}e^{-2}\text{IM}) = 3.0$ ps was modeled and depicted in Fig. 4. It shows spectra of the incident pulse (upper curve) and of the recompressed pulse (lower curve). One can see that for a CBG with spectral width $\Delta\lambda(\text{FW}) \approx 0.1$ nm equal to that of a laser pulse at the level of $1/e^2$, the spectral width of a recompressed pulse is practically the same. However, there is some modulation of the spectrum in the vicinity of the maximum, which is caused by ripples in the dispersion curve depicted in Fig. 3; cutting off short- and long-wavelength wings of the spectrum and the spectral width of the CBG is due to finite spectral width of CBG.

Figure 5 shows the intensity profiles of the input pulse, stretched pulse (multiplied by factor 80 for illustrative
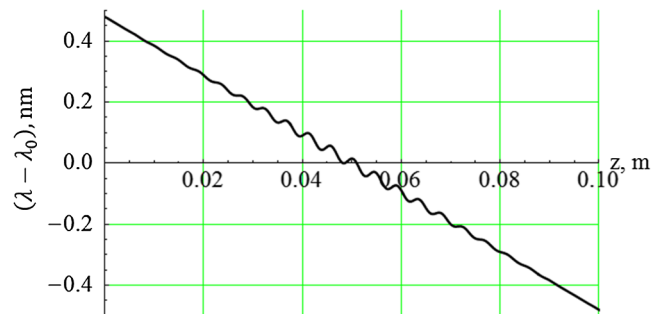


**Fig. 3** Dependence of Bragg resonant wavelength detuning on position inside CBG. Particular perturbation of the phase is given by Eq. (39) with top-to-bottom modulation $2a = 0.4$ rad. Given wavelength corresponds to one or three resonant points.
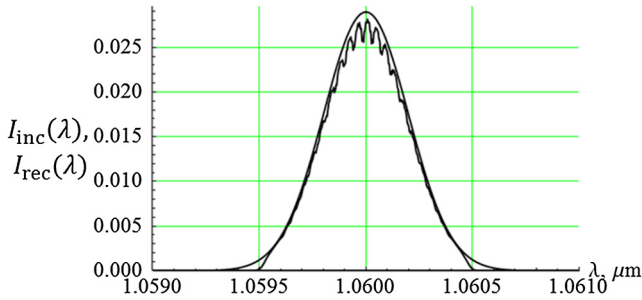
**Fig. 4** Spectra of Fourier transform–limited incident pulse (upper curve) and of recompressed pulse (lower curve); time duration of input pulse $\Delta t$ (HW$e^{-2}$IM) = 3 ps.

purposes), and recompressed pulse for CBG with the above oscillatory perturbations of the phase $\delta\psi(z)$ of the grating. Input pulse was a transform-limited Gaussian pulse with $\Delta t$(HW$e^{-2}$IM) = 3 ps. The properties of CBG are the same as for Figs. 3 and 4. There is a small precursor in the recompressed pulse (arrow in Fig. 5) containing ~6% of recompressed energy. Nevertheless one observes rather good quality of recompression: diffraction efficiency of full cycle of stretching–compression for energy was 0.92 and ratio of peak intensities was 0.61. It means that steep perturbation of phase $\delta\psi$ with amplitude $2a \lesssim 0.4$ rad is not harmful for recompression. Meanwhile, our modeling for perturbations with amplitude $2a \gtrsim 0.4$ rad had shown considerable hindering recompression.

### 5.3 Study of Time-Delay Dispersion

For the evaluation of our analytic (but approximate) results for time-delay dispersion, TDD($\lambda$), we had to choose a special approach in numerical modeling. Namely, illumination of CBG by a very short incident pulse (< 1 ps and therefore with a very broad spectrum) resulted in a stretched pulse with very flat top, for which it was difficult to find TDD at the stretching stage. If any distortions in the temporal profile of stretched pulse were present, the arrival time of the peak of reflected pulse was difficult to determine. On the other hand, if the incident pulse was relatively long (and hence was relatively narrow-band), the reflected pulse was not stretched to full possible duration $2L/v_{gr}$. Here $v_{gr}$ is the group velocity at $\lambda_0$ in unexposed glass. Still, determining the delay time for stretching stage was difficult due to large duration of the input pulse.

For that reason we calculated from numerical wave modeling the delay time of a recompressed pulse in comparison with the arrival time of an incident pulse. The delivery of the stretched pulse to the back of CBG for recompression was considered to be instantaneous in the modeling. Two types of CBG were considered. One type was with $|\kappa| = S/L$ taken as a constant through the whole thickness $L$ of CBG; hereafter, we call this type of CBG as uniform or nonapodized. The other type had the profile

$$|\kappa(z)| = \frac{S}{L} \cdot \text{apod}(z); \quad \text{apod}(z) = 1 - \left(\frac{2z}{L} - 1\right)^{10}. \quad (40)$$

This apodization function suppressed not-quite Bragg contributions of the ends of CBG; the latter contribution leads to Fresnel function-like oscillations in the reflection spectrum of nonapodized CBG. For both cases we calculated TDD (at $\lambda_0 = 1.06$ $\mu$m) for different values of dimensionless parameter $S$ (and for constant chirp $\beta = 8 \cdot 10^4$ rad/m$^2$). The results for TDD slightly varied as a function of duration of input Gaussian pulse $\tau_0$ (HW$e^{-2}$IM). The shortest pulse duration $\tau_0$, for which this CBG still reflected almost all the spectrum, was $\tau_0 = 3.0$ ps. The stretched pulse in both cases had a duration of ~1 ns, i.e., 300 times longer than the input one.

Figure 6 shows the comparison of numerical modeling of time-delay $T_{cycle}$ with our analytic approximation, Eqs. (27), (28), and (33). The square points in Fig. 6 show full duration of stretching–recompression process versus dimensionless coupling coefficient $S = |\kappa|L$ for unapodized CBG. Triangular points describe corresponding data for apodized CBG. Dashed and dotted lines are calculated by the analytic model [Eqs. (27) and (28)]. Parabolic curve describing the simple formula [Eq. (33)] (not shown) is almost the same
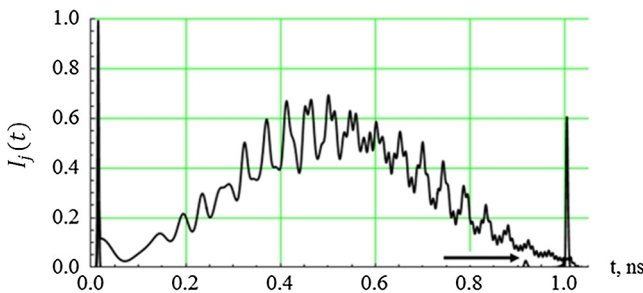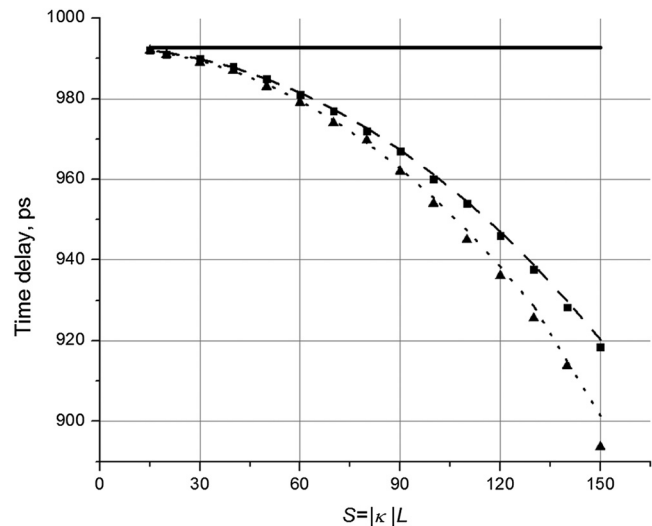


**Fig. 5** Intensity profiles of input pulse (left), stretched pulse (multiplied by factor 80 for illustrative purposes, center), and recompressed pulse (right) for CBG with oscillatory perturbations of phase $\delta\psi(z)$ of the grating. Arrow points to a precursor in the recompressed pulse containing ~6% of its energy.



**Fig. 6** Dependence of total time-delay between incident short pulse [Gaussian, with $\Delta t$ [(HW$e^{-2}$IM) = 12 ps] and recompressed pulse on the dimensionless coupling coefficient $S = |\kappa|L$. Square and triangular points correspond to numerical modeling of unapodized and apodized CBG, respectively. Dashed and dotted lines for corresponding CBG yield the results calculated by analytic model Eqs. (27) and (28). Parabolic curve describing simple formula Eq. (33) (not shown) is almost the same as dashed curve for unapodized CBG. We see quadratic deviation of those curves from $2L/v_0$ (from horizontal line) versus coupling $|\kappa| = S/L$.
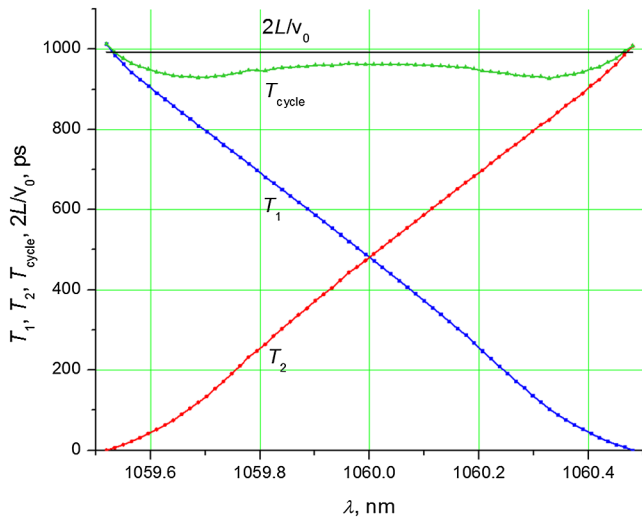
**Fig. 7** Dependence of stretching time $T_1(\lambda)$ calculated by Eq. (27) for apodized CBG with $S = 90$, compression time $T_2(\lambda)$, Eq. (28), time of cycle stretching–compression $T_{cycle}(\lambda) = T_1(\lambda) + T_2(\lambda)$, time of double pass through blank glass $2L/v_0$.

as the dashed curve for unapodized CBG. We see quadratic deviation of those curves from $2L/v_0$ (form horizontal line) versus coupling $|\kappa| = S/L$. All data are for the input pulses with $\tau_0 = 12.0$ ps at the central wavelength $\lambda_0 = 1.06~\mu$m of our CBG. We see that the approach used in the derivation of the integrals [Eqs. (27), (28), and (33)] yields very reasonable correspondence with the results of numerical modeling.

Here is an important (and originally unexpected) observation. Too large a value of coupling ($S \geq 70$) for that particular CBG and $\tau_0 = 3.0$ ps, while yielding 99.4% diffraction efficiency for energy of recompressed pulse, resulted in relatively poor quality of recompression: peak intensity of recompressed pulse constituted 52% of the incident one. Our interpretation of that decrease of recompression quality is the following. Different spectral components of incident pulse exhibit somewhat different values of the sum $T_{cycle}(\lambda) = T_1(\lambda) + T_2(\lambda)$, from integrals [Eqs. (27) and (28)] with different values of $z_B(\lambda)$, see Fig. 7 for apodized CBG with $S = 90$. The presence of shorter values of $T_{cycle}(\lambda)$ points to the formation of precursor in the recompressed pulse. This effect leads to deteriorated recompression. Meanwhile, the fact that two considerably distant wavelengths have those shorter values of $T_{cycle}(\lambda)$ explains interference-type oscillations in the precursor.

## 6 Conclusions

We have developed a detailed Mathematica-based numerical tool for modeling the process of stretching–recompression by CBG with arbitrary profiles of the grating's phase and coupling coefficient. To better understand the results of numerous variants of that modeling, we developed approximate analytical model of time-delay dispersion TDD($\lambda$). An unexpected result of that analytic model is that dependence of TDD on the coupling constant $|\kappa| = S/L$ starts with terms proportional to $|\kappa|^2$. We have shown that excessively large coupling in CBG leads to deterioration of recompression

quality. We show that perturbations of grating phase with small ($< \sim 0.4$ rad top-to-bottom) amplitude do not hinder the recompression quality much, enabling >90% of energy in the recompressed pulse.

## References

1. E. B. Treacy, "Optical pulse compression with diffraction gratings," *IEEE J. Quantum Electron.* **5**(9), 454–458 (1969).
2. A. Galvanauskas et al., "All-fiber femtosecond pulse amplification circuit using chirped Bragg gratings," *Appl. Phys. Lett.* **66**(9), 1053–1055 (1995).
3. W. Chang et al., "Femtosecond pulse spectral synthesis in coherently-spectrally combined multi-channel fiber chirped pulse amplifiers," *Opt. Express* **21**(3), 3897–3910 (2013).
4. K.-H. Liao et al., "Large-aperture chirped volume Bragg grating based fiber CPA system," *Opt. Express* **15**(8), 4876–4882 (2007).
5. L. B. Glebov, "Volume holographic elements in a photo-thermo-refractive glass," *J. Hologr. Speckle* **5**(1), 77–84 (2009).
6. G. Chang et al., "Femtosecond Yb-fiber chirped-pulse-amplification system based on chirped-volume Bragg gratings," *Opt. Lett.* **34**(19), 2952–2954 (2009).
7. O. V. Belai, E. V. Podivilov, and D. A. Shapiro, "Group delay in Bragg grating with linear chirp," *Opt. Commun.* **266**(2), 512–520 (2006).
8. L. Poladian, "Graphical and WKB analysis of nonuniform Bragg gratings," *Phys. Rev. E* **48**(6), 4758–4767 (1993).
9. L. D. Landau and E. M. Lifshitz, *Quantum Mechanics: Non-Relativistic Theory*, §50, problem 4, Pergamon Press, Oxford (1977).
10. L. Glebov, "Fluorinated silicate glass for conventional and holographic optical elements," *Proc. SPIE* **6545**, 654507 (2007).
11. L. Glebov et al., "Volume chirped Bragg gratings—monolithic components for stretching and compression of ultrashort laser pulses," *Opt. Eng.*

**Sergiy Kaim** graduated from Mechnikov Odessa University in 2006, where he received his MS degree in physics. Since 2008, he is pursuing his PhD in physics at the University of Central Florida, where his research interests are in the areas of laser beam quality characterization, efficiency and quality of laser beam combination, and properties of volume Bragg gratings.

**Sergiy Mokhov** graduated from the department of theoretical physics of Kiev University in Ukraine in 1996. Then he pursued his PhD in nuclear physics at that university. In 2004, he moved to CREOL–the College of Optics at the University of Central Florida. From 2006, he has worked with Professor B. Zeldovich and Professor L. Glebov's group on the theory of volume Bragg gratings. He earned his PhD in optics from CREOL in 2011.

**Boris Y. Zeldovich** graduated from Moscow University in 1966 and received his doctor of physical and mathematical sciences degree from the Lebedev Physics Institute in Moscow, Russia. He is currently a professor of optics and physics at the University of Central Florida's CREOL College of Optics and Photonics. He is the codiscoverer of optical phase conjugation. He is a member of the Russian Academy of Science and won the 1997 Max Born award for physical optics from OSA.

**Leonid B. Glebov** got his PhD from the State Optical Institute, Leningrad, Russia (1976). Since 1995, he has been at CREOL, University of Central Florida, as a research professor. He is a founder and VP of OptiGrate Corp. He is the coauthor of a book, 300+ scientific articles, and 10 patents. He is a fellow of ACerS, OSA, SPIE, and NAI. He is a recipient of a Gabor award in holography. His main directions of research are glasses, holography, and lasers.